Bull. Mater. Sci., Vol. 32, No. 2, April 2009, pp. 177–181. © Indian Academy of Sciences.

Effects of talc and clay addition on pressureless sintering of porous Si_3N_4 ceramics

YU FANGLI, YANG JIANFENG*, XUE YAOHUI[†], DU JUN[#], LU YUAN and GAO JIQIANG

State Key Laboratory for Mechanical Behaviour of Materials, Xi'an Jiaotong University, Xi'an 710049, P.R. China
[†]The School of Electronic and Information Engineering, Xi'an Jiaotong University, Xi'an 710049, P.R. China
[††]National Key Laboratory of Remanufacture, No. 21, DuJiaKan, ChangXinDian, Beijing 100072, P.R. China

MS received 21 July 2008; revised 15 September 2008

Abstract. **Porous Si_3N_4 ceramics were successfully synthesized using cheaper talc and clay as sintering additives by pressureless sintering technology and the microstructure and mechanical properties of the ceramics were also investigated. The results indicated that the ceramics consisted of elongated β-Si_3N_4 and small Si_2N_2O grains. Fibrous β-Si_3N_4 grains developed in the porous microstructure, and the grain morphology and size were affected by different sintering conditions. Adding 20% talc and clay sintered at 1700°C for 2 h, the porous Si_3N_4 ceramics were obtained with excellent properties. The final mechanical properties of the Si_3N_4 ceramics were as follows: porosity, $P_0 = 45{\cdot}39\%$; density, $\rho = 1{\cdot}663\,\text{g}\cdot\text{cm}^{-3}$; flexural strength, σ_b (average) = 131·59 MPa; Weibull modulus, $m = 16{\cdot}20$.**

Keywords. **Talc; clay; pressureless sintering; porous Si_3N_4; mechanical properties; Weibull distribution.**

1. Introduction

Porous ceramic materials have many industrial applications as filtering materials including uses as high temperature gas filters, separation membranes, bioreactors and catalyst supports (Zaman and Chakma 1994; Jonker and Potgieter 2005). In particular, porous Si_3N_4 ceramics with elongated β-Si_3N_4 grains show superior mechanical properties, such as high strength, good thermal shock resistance (Arnold *et al* 1996; Shigegaki *et al* 1997), high strain and damage tolerance (Kawai and Yamakawa 1997; Inagaki *et al* 2000). In general, for the densification of porous Si_3N_4 ceramics, the liquid phase sintering is carried out using different sintering additives such as MgO, Al_2O_3, Y_2O_3, Yb_2O_3 and other rare oxides or their combination (Kawai and Yamakawa 1998; Yang *et al* 2000, 2006; Lee and Kim 2004). However, to minimize the cost of Si_3N_4 ceramics, the choice of sintering additive with reasonable costs as well as decreasing the sintering temperature are required, especially, for the application of intermediate temperature. In this point of view, the cheaper talc and clay, which are aluminosilicates containing different amounts of calcium, potassium, or sodium can be considered as low temperature and low cost sintering additives. In the glass ceramics, the talc and clay was widely used as a flux to decrease the vitrifying temperature of ceramics during firing and forming a glassy phase. Compared to other additives, the talc and clay additives offered an opportunity to reduce the cost of Si_3N_4 ceramics.

In this work, porous Si_3N_4 ceramics were successfully synthesized with α-Si_3N_4 as starting materials and the cheaper talc and clay as sintering additives by pressureless sintering technology. The effects of the talc and clay on the ceramics phase composition, microstructure and mechanical properties were investigated.

2. Experimental

2.1 *Preparation of samples*

Commercial α-Si_3N_4 powder (Shanghai Junyu Co. Ltd., Shanghai, China; α-Si_3N_4 ratio: >95%, mean particle size: 1·2 μm, main impurities by weight: O = 1·6%; C < 0·2%; Cl, Fe, Ca, and Al_2O_3 < 80 ppm) was used as the starting powder, and various contents (10–40 wt%) of talc and clay with a weight ratio of 8 : 2 were used as sintering additives. The chemical compositions of talc and clay given in weight percentages of oxides are given in table 1. The compositions of test samples are listed in table 2.

The mixtures were wet-milled in methanol for 24 h, using high-purity Si_3N_4 media. The obtained slurry was dried and sieved through a 150 μm screen. The mixed powders were then pressed under 20 MPa, to form rectangular bars measuring 55 × 6 × 5 mm. The green bodies were placed in a BN-coated graphite crucible and sintered

*Author for correspondence (yang155@mail.xjtu.edu.cn)

Table 1. Chemical compositions of talc and clay.

Raw materials	Compositions (wt%)								
	SiO_2	Al_2O_3	Fe_2O_3	TiO_2	CaO	MgO	K_2O	Na_2O	Ignition loss
Talc	60·44	0·27	0·34	–	1·07	30·37	–	–	3·32
Clay	46·00	35·90	0·95	0·03	0·40	0·01	0·21	0·02	4·96

Table 2. Compositions of the starting raw materials of samples.

Samples	Composition (wt%)
*S*1	90% α-Si_3N_4 + 10% talc and clay
*S*2	80% α-Si_3N_4 + 20% talc and clay
*S*3	70% α-Si_3N_4 + 30% talc and clay
*S*4	60% α-Si_3N_4 + 40% talc and clay

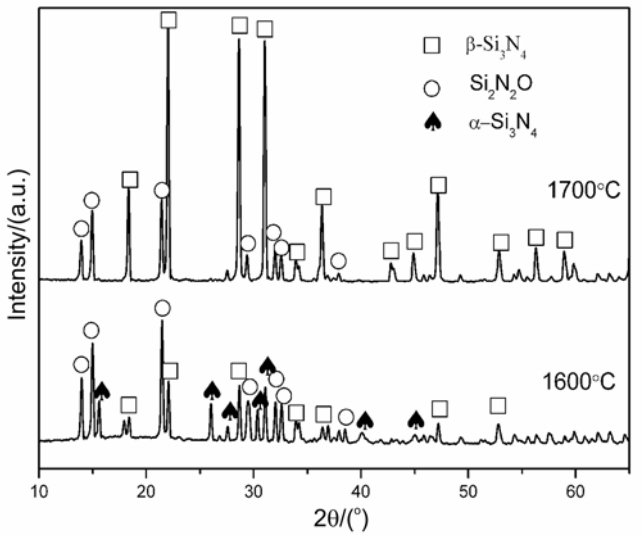

Figure 1. XRD patterns of sample, *S*2, sintered at 1600°C and 1700°C.

in graphite resistance furnace (High multi-5000 Fijidempa Co. Ltd., Osaka, Japan) at various temperatures under a nitrogen–gas pressure of 0·3 MPa. The heating rate was 10–20°C/min and holding time was 2 h.

2.2 *Examination of properties*

The three-point bending strength was measured on sample bars with a span of 16 mm at a crosshead speed of 0·5 mm/min by an instrument (model Instron 1195, Instron Co., Buckinghamshire, England). Each final value was averaged over five measurements.

The bulk density of the sintered products was measured by the Archimedes displacement method. Crystalline phases were identified by an X-ray diffractometry (XRD, D/MAX-2400X, Rigaku Co., Tokyo, Japan) analysis. Microstructure was characterized by a scanning electron microscope (SEM, JSM-35C, JEOL, Tokyo, Japan).

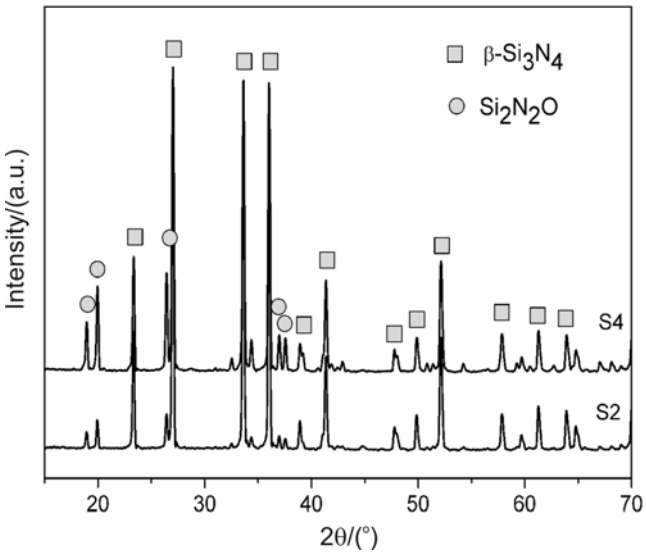

Figure 2. XRD patterns of samples, *S*2 and *S*4.

3. Results and discussion

3.1 *Phase composition and microstructure*

The XRD results of the sample, *S*2, are shown in figure 1. It could be seen that peaks of β-Si_3N_4, Si_2N_2O and α-Si_3N_4 could be observed, the α–β Si_3N_4 phase transformation could not take place completely when sintered at 1600°C, so that a mass of α-Si_3N_4 remained in the sample, and it was noticed that comparatively strength of Si_2N_2O were detected together with β-Si_3N_4 and α-Si_3N_4 phases. Si_2N_2O and β-Si_3N_4 existed by the α/β phase transformation of Si_3N_4. Heated at 1700°C, the reaction took place completely, so that β-Si_3N_4 and Si_2N_2O were detected.

The XRD patterns of samples *S*2 and *S*4 sintered at 1700°C for 2 h are shown in figure 2. The main phase was β-Si_3N_4, implying an almost complete α–β phase transformation, and the secondary phase was Si_2N_2O alone, the formation of Si_2N_2O phase was reported in the phase relation of Si_3N_4–SiO_2–Al_2O_3 systems at high temperature (Mitomo *et al* 1989). With an increase in talc and clay, the amount of Si_2N_2O increased.

The microstructures of sample, *S*2, sintered at 1600 and 1700°C are shown in figure 3. The microstructure of the sample, *S*2, sintered at 1600°C consisted of fine and equiaxed grains (figure 3 (a)). The average grain size was

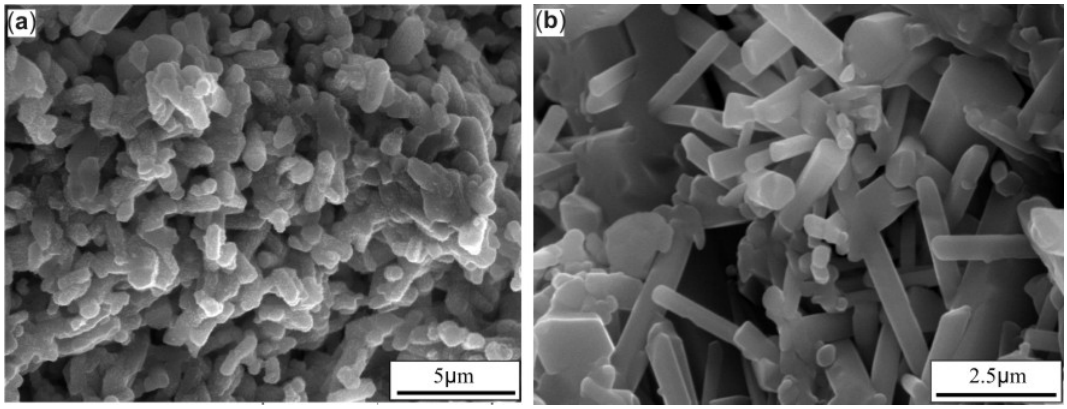

Figure 3. SEM images of sample, *S*2, sintered at 1600°C (**a**) and 1700°C (**b**).

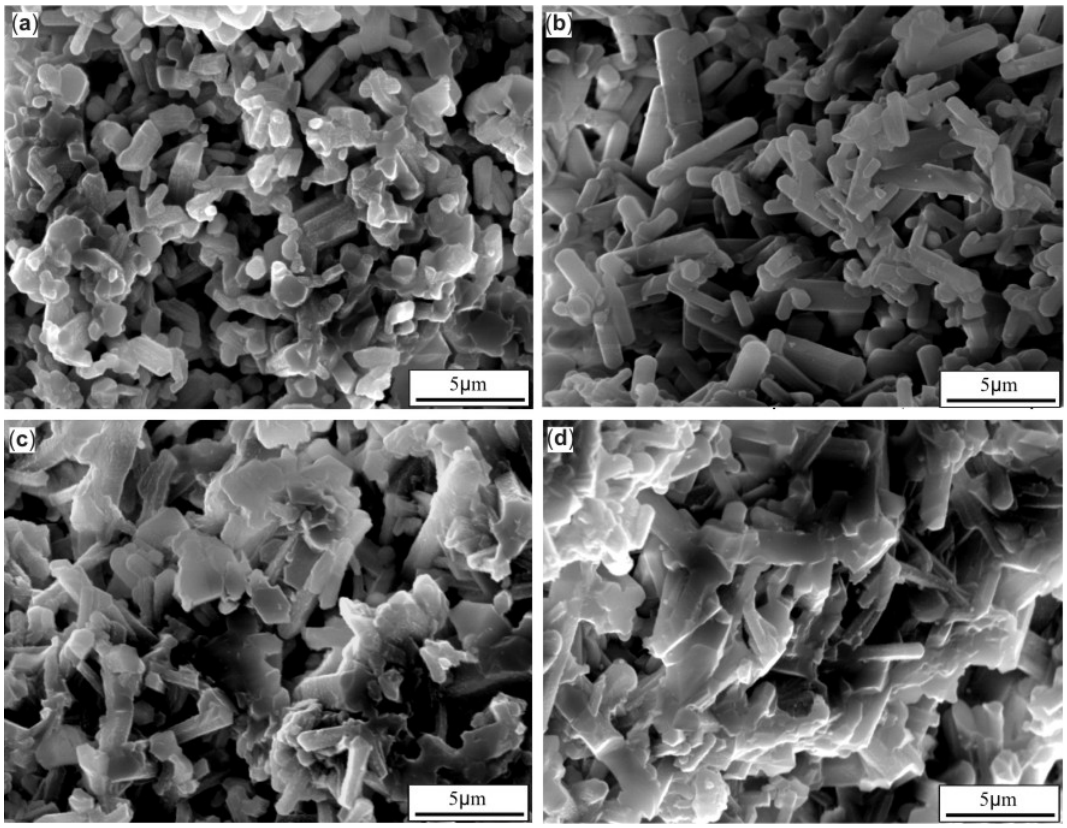

Figure 4. SEM images of porous Si_3N_4 ceramics: (**a**) *S*1, (**b**) *S*2, (**c**) *S*3 and (**d**) *S*4. The samples were sintered at 1700°C for 2 h.

almost the same as that of the starting powder, indicating part phase transformation, which could also be confirmed by XRD analysis as α-Si_3N_4 peaks were identified. Because the density after sintering exhibited part change, complete sintering was not achieved at this temperature. Increasing the sintering temperature caused the formation and development of β-Si_3N_4 grains, indicating enhanced phase transformation and grain growth. When the sample, *S*2, was sintered at 1700°C, very fine, fibrous β-Si_3N_4 grains were obtained (figure 3 (b)).

Figure 4 shows microstructures of Si_3N_4 ceramics with varying additive contents. From figure 4(a), fine equiaxial β-Si_3N_4 grains could be seen. Increasing the talc and clay content resulted in the formation of large, elongated Si_3N_4 grains in the fine matrix, as shown in figure 4(b). However, that with a large additive content exhibited a coarse and conglomerated Si_3N_4 grains (figures 4(c), (d)). The explanation could be given by the following reasons. Densification and α–β phase transformation were two phenomena which occurred during the sintering of Si_3N_4

Table 3. Mechanical properties of Si_3N_4 ceramics sintered sample, *S*2, at 1600 and 1700°C.

Temperature (°C)	Porosity (%)	Density ($g \cdot cm^{-3}$)	Relative density (%)	σ_b (average) (MPa)
1600	40·87	1·534	48·12	76·30
1700	45·39	1·663	52·13	131·59

ceramics. For liquid phase sintering, an effective liquid phase with a sufficient volume fraction, good wettability to solid phase and appreciable solubility of the solid was required. Both the densification and phase transformation were greatly influenced by the type and amount of the liquid phase. According to $MgO–Al_2O_3–SiO_2$ phase diagram, most of the components of the talc and clay powder could be changed into an amorphous phase at 1355°C. With the additive content, the densification was achieved due to particle rearrangement and with a small additive content, and it was achieved due to particle rearrangement and coalescence. This speculation was supported by the result that the densification depended strongly on the sintering additive content due to the fact that a large amount of the boundary liquid phase facilitates the particle rearrangement. The phase transformation and grain growth in Si_3N_4 ceramics was controlled by the diffusion mechanism through the liquid grain-boundary film, or the interface reaction (Lifzhitz and Slyozov 1961; Hampshire and Jack 1983). The main factor that determined the rate-controlling mechanism was the diffusion velocity of Si and N atoms in the liquid phase, the interface reaction rate-controlling for high diffusion velocity and diffusion controlling for low diffusion velocity. Sintering additives affected these behaviours through the glass phase (Emoto *et al* 1999). However, the phase transformation and grain growth were suppressed by the large increase in the talc and clay contents. The large additive content resulted in a high viscosity of the liquid phase in the $MgO–Al_2O_3–SiO_2$, this led to slower diffusion rate for Si and N through the liquid phase, and thus, the phase transformation and grain growth were retarded.

3.2 *Mechanical properties*

The mechanical properties of the sample, *S*2, sintered at 1600 and 1700°C are listed in table 3. When the sample, *S*2, was sintered at 1600°C, at which little phase transformation occurred, the flexural strength was very low. Usually, phase transformation starts in the temperature range 1600~1650°C, and grain growth starts at the same time. Of course, increasing the sintering temperature will accelerate the development of large, elongated grains. In the present study, high strength was obtained for the sample, *S*2, sintered at 1700°C, which indicated that fine-sized, fibrous Si_3N_4 grains, rather than coarse grains, favour high strength in porous Si_3N_4 ceramics, which was in accordance with the SEM above.

Table 4 exhibits the porosity, density and flexural strength of Si_3N_4 ceramics. Clearly, the flexural strength decreased as porosity increased. The sample, *S*2, with 20% talc and clay contents exhibited excellent properties. This could be explained as being due to the coexisting effects between the microstructure and the remaining glass phase. Fibrous β-Si_3N_4 grains were known to enhance the flexural strength of Si_3N_4 ceramics (Yang *et al* 2001), most likely because the fibrous β-Si_3N_4 grains were beneficial for strengthening by grain bridging and pullout. With increasing additive content, the matrix grains were refined, but the amount of the grain-boundary glassy phase increased, it was very likely that the former increased the flexural strength while the latter decreased it.

3.3 *Weibull distribution*

For a given ceramic material the distribution of crack size, shape, and orientation differs from sample to sample. It is experimentally reported that the strength of ceramics varies unpredictably even if identical specimens are tested under identical loading conditions. For analysing flexural strength distribution of the ceramics material, Weibull (1951) proposed a two-parameter distribution function to characterize the strength of brittle materials. The Weibull distribution function has the following expression:

$$P(\sigma) = 1 - \exp\left[-\left(\frac{\sigma}{\sigma_0}\right)^m\right], \quad (1)$$

where $P(\sigma)$ is the probability of failure at a given stress level 'σ', m the Weibull modulus and σ_0 the scale parameter. The characteristic strength distribution parameter, m, indicates the nature, severity and dispersion of flaws. More clearly, a low m value indicates non-uniform distribution of highly variable crack length (broad strength distribution), while a high m value implicates uniform distribution of highly homogeneous flaws with narrower strength distribution. Typically, for structural ceramics, m varies between 5 and 30, depending on the processing conditions (Bazant 2004), so the Weibull distribution function is widely used to characterize the fracture strength of the porous Si_3N_4 ceramics. Figure 5 shows Weibull statistics analysis where failure probability was plotted vs applied load. This value clearly indicated that these ceramics had comparatively higher flexural strength.

Table 4. Mechanical properties of Si_3N_4 ceramics.

Sample	Porosity (%)	Density (g·cm^{-3})	Relative density (%)	σ_b (average) (MPa)
*S*1	46·78	1·582	49·61	103·30
*S*2	45·39	1·663	52·13	131·59
*S*3	41·88	1·683	52·77	114·22
*S*4	12·54	2·659	68·45	184·09

Table 5. Weibull modulus (m) of the samples.

Samples	*S*1	*S*2		*S*3	*S*4
Weibull modulus, m	13·71	1600 (°C) 7·419	1700 (°C) 16·20	14·03	12·25

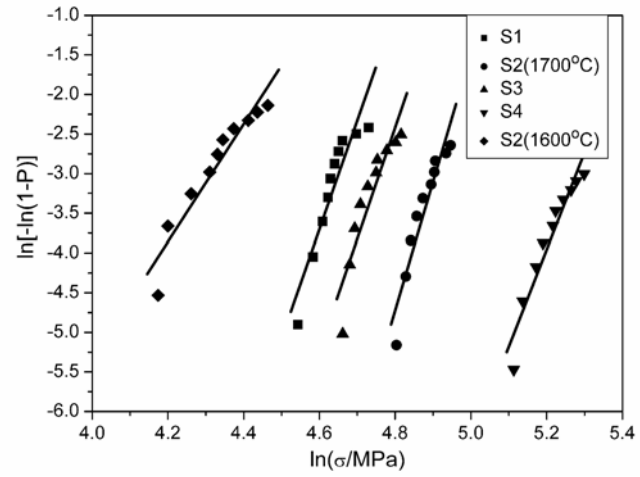

Figure 5. Weibull statistics analysis results of the samples.

All the strength data i.e. datasets *S*1, *S*2, *S*3 and *S*4, are tabulated in table 5. For *S*2 sintered at 1700°C, it could be noted that the Weibull modulus (m) was very high, which indicated uniform distribution of highly homogeneous flaws with narrower strength distribution in sample, *S*2, sintered at 1700°C. Adding 20% talc and clay in the starting powders sintered at 1700°C for 2 h, porous Si_3N_4 ceramics were successfully synthesized with excellent properties.

4. Conclusions

(I) Using α-Si_3N_4 as starting material, and the cheaper talc and clay as sintering additives, porous Si_3N_4 ceramics were fabricated by pressureless sintering technology, and the composite ceramics consisted of fine, fibrous β-Si_3N_4 and small Si_2N_2O grains.

(II) The mechanical properties were obtained by adjusting the sintering conditions and additive content. Adding 20% talc and clay in the starting powders sintered at 1700°C for 2 h, porous Si_3N_4 ceramics were successfully synthesized with excellent properties. The final mechanical properties of the Si_3N_4 ceramics were as follows: porosity, $P_0 = 45{\cdot}39\%$; density, $\rho = 1{\cdot}663$ g·cm^{-3}; flexural strength, σ_b (average) = 131·59 MPa; Weibull modulus, $m = 16{\cdot}20$.

Acknowledgements

This work was supported by the Ministry of Education of the People's Republic of China within the Program for New Century Excellent Talents in University (NCET-04-0941), and by the Research Fund for the Doctoral Program of National Ministry, Higher Education, under contract no. 20060698008.

References

Arnold M, Boccaccini A R and Ondracek G 1996 *J. Mater. Sci.* **31** 463
Bazant Z P 2004 *Prob. Eng. Mech.* **19** 307
Emoto H, Hirotsuru H and Mitomo M 1999 *Key Eng. Mater.* **159–160** 215
Hampshire S and Jack K H 1983 *Progress in nitrogen ceramics* (ed.) F L Riley (The Hague: Martinus Nijhoff Publisher) pp 225–230
Inagaki Y, Ohji T, Kanzaki S and Shigegaki Y 2000 *J. Am. Ceram. Soc.* **83** 1807
Jonker A and Potgieter J H 2005 *J. Eur. Ceram. Soc.* **25** 3145
Kawai C and Yamakawa A 1997 *J. Am. Ceram. Soc.* **80** 2705
Kawai C and Yamakawa A 1998 *Ceram. Int.* **24** 135
Lee B T and Kim H D 2004 *Mater. Sci. Eng.* **A364** 126
Lifzhitz I M and Slyozov V V 1961 *J. Phys. Chem. Solids* **19** 35
Mitomo M, Ono S and Asami T 1989 *Ceram. Int.* **10** 14
Shigegaki Y, Brito M E, Hirao K, Toriyama M and Kanzaki S 1997 *J. Am. Ceram. Soc.* **82** 495
Weibull W 1951 *J. Appl. Mech.* **18** 293
Yang J F, Ohji T and Niihar A K 2000 *J. Am. Ceram. Soc.* **83** 2094
Yang J F, Zhang G J and Ohji T 2001 *J. Am. Ceram. Soc.* **84** 1639
Yang J, Yang J F, Shan S Y, Gao J Q and Ohji T 2006 *J. Am. Ceram. Soc.* **89** 3843
Zaman J and Chakma A 1994 *J. Membr. Sci.* **92** 1